AJNR

Visualization of Microvascularity in Glioblastoma Multiforme With 8-T High-Spatial-Resolution MR Imaging

Gregory A. Christoforidis, John C. Grecula, Herbert B. Newton, Allahyar Kangarlu, Amir M. Abduljalil, Petra Schmalbrock and Donald W Chakeres

AJNR Am J Neuroradiol 2002, 23 (9) 1553-1556
http://www.ajnr.org/content/23/9/1553

AJNR Am J Neuroradiol 23:1553–1556, October 2002

Technical Note

Visualization of Microvascularity in Glioblastoma Multiforme With 8-T High-Spatial-Resolution MR Imaging

Gregory A. Christoforidis, John C. Grecula, Herbert B. Newton, Allahyar Kangarlu, Amir M. Abduljalil, Petra Schmalbrock, and Donald W Chakeres

Summary: We used 8-T high-spatial-resolution gradient-echo MR imaging to directly visualize microvascularity in pathologically proved glioblastoma multiforme. Images were compared with 1.5-T high-spatial-resolution fast spin-echo T2-weighted images and digital subtraction angiograms. Preliminary data indicate that 8-T high-spatial-resolution MR imaging may enable the identification of areas of abnormal microvascularity in glioblastoma multiforme that are not visible with other routine clinical techniques.

Angiogenesis in an astrocytic neoplasm is a feature of a more aggressive tumor such as a glioblastoma multiforme, and histopathologic methods based on the number of vessels, degree of glomeruloid vascular formation, and endothelial cytology have been used to grade it (1, 2). More recently, microvascular density analysis with panendothelial staining techniques (eg, with factor VIII or CD34) has been used to quantify angiogenesis and has been found to act as an independent predictor of disease-free survival (3, 4). Other investigators have suggested that imaging findings of vascular density in a tumoral bed may, in theory, act as an indicator for tumoral angiogenesis (5–7). In this context, the purpose of this study was to directly identify the microvascular features of glioblastoma multiforme at 8 T and to correlate those features with imaging findings at 1.5 T and conventional catheter digital subtraction angiography (DSA).

Description of the Technique and Results

A 37-year-old man had a glioblastoma multiforme of the left parietal lobe that was examined at stereotactic biopsy. The patient underwent 8-T MR imaging after providing written informed consent. The protocol was performed with approval of our institutional review board and in accordance with a consent form under an Food and Drug Administration–approved Investigational Device Exemption. Images were acquired by using a commercial console (Bruker Avance; Bruker, Billerica, MA) and a custom-built radio-frequency (RF) front end (8). A modified two-port, quadrature-drive, 16-strut, transverse, electromagnetic, RF volume coil (8) was individually tuned on the head of the patient. The head coil was placed inside the bore of the 8-T, 80-cm magnet (GE Magnex Scientific, Abingdon, England). A conventional two-dimensional, multisection, gradient recalled-echo sequence was used to encode the images. RF spoiling and 250 ìs of gradient spoiling along the section direction reduced the residual transverse coherence. Images were acquired in 2-mm sections in the axial plane with a 20-cm field of view FOV and encoded into square 900×900-pixel matrices. As such, the in-plane pixel size was 222 μm. A TR of 714 ms was selected to maintain a reasonable imaging time of 10 minutes 49 seconds with an adequate signal-to-noise ratio. To increase the degree of contrast and T2* weighting, the nutation angle was set to approximately 23°, and the TE was set to 10 ms. These parameters were derived from the solutions to the Bloch equations for the spoiled gradient-echo sequence and from the preliminary 8-T relaxation parameter estimates. An FOV of 20 cm was used, and 24 sections were acquired with an NEX of 1.

The patient also underwent imaging at 1.5 T performed with a commercial system (Signa LXCV; GE Medical Systems, Milwaukee, WI). Fast spin-echo (FSE) T2-weighted axial images were acquired with a TR/TE of 5650/104, an FOV of 20 cm, a matrix of 512×512, and a section thickness of 3 mm. These images were compared with the 8-T MR images obtained on the same date. Foci of microvascularity were then identified on the 8-T images, and the corresponding regions were identified on the 1.5-T images (Fig 1). The size of the vessels identified at 8 T was compared with the size of cortical penetrating veins. To identify vessels beyond the resolution of 8-T imaging, the signal intensity immediately adjacent to the foci of visible tumoral microvascularity was measured and compared with the signal intensity of the tumoral bed excluding these foci. For this comparison, we used NIH Image software version 1.62 (National Institutes of Health, Bethesda, MD; available at *rsb.info.nih.gov/nih-image*) (Fig 1).

Foci of enlarged vasculature and foci of tortuous vascularity in the tumoral bed were identified on the 8-T images, and their size was compared with the size of the cortical penetrating veins in the same patient. The ratio of the sum of the diameters of three transmedullary veins adjacent to the tumoral bed to the sum of the diameters of three transmedullary veins away from the tumoral bed was also calculated.

The patient began intraarterial chemotherapy. As part of this treatment, DSA was performed by using a biplane Neurostar TOP system (Siemens, Erlangen, Germany). The arteriograms were evaluated for areas of increased vascularity, increased vascular size, and vascular blush. The arteriographic images were then compared with the 8-T MR images to identify similar vascular features and to help validate the

Received October 26, 2001; accepted after revision May 14, 2002.

From the Departments of Radiology (G.A.C., J.C.G., A.K., A.M.A., P.S., D.W.C.) and Neurology (H.B.N.), the Ohio State University Medical Center, Columbus.

Address reprint requests to Gregory A. Christoforidis, M.D., Assistant Professor, Department of Radiology, the Ohio State University Medical Center, 168 Means Hall, 1654 Upham Drive, Columbus, OH 43221.

Supported by the National Cancer Institute (U01 CA 76576–03), the National Cancer Institute (P30 CA16058), the National Institutes of Health (M01 RR00034), and Pharmacyclics, Inc.

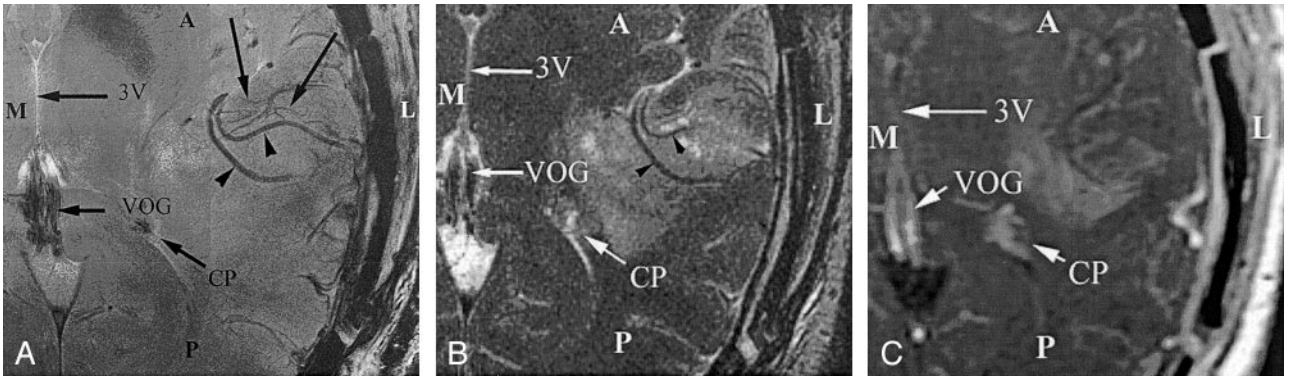

FIG 1. Comparison of MR images obtained at the inferior border of a glioblastoma multiforme. Although the arterial structures in the sylvian fissure (*arrowheads*) are identified at both 1.5- and 8-T imaging, the smaller venous structures (*unlabeled arrows*) are depicted only on the 8-T image. These venous structures represent draining veins from the tumoral bed. *A* indicates anterior; *CP*, choroid plexus within the trigone of the left lateral ventricle; *L*, lateral; *M*, medial; *P*, posterior; *VOG*, vein of Galen; and *3V*, third ventricle.

A, Image obtained at 8 T (714/10, 23° flip angle, 900 × 900 matrix, 2-mm section thickness, 20-cm FOV).

B, FSE T2-weighted image obtained at 1.5 T (5650/104, 512 × 512 matrix, 3-mm section thickness, 20-cm FOV).

C, Gadolinium-enhanced magnetization-transfer image obtained at 1.5 T (616/20, 256 × 256 matrix, 5-mm section thickness).

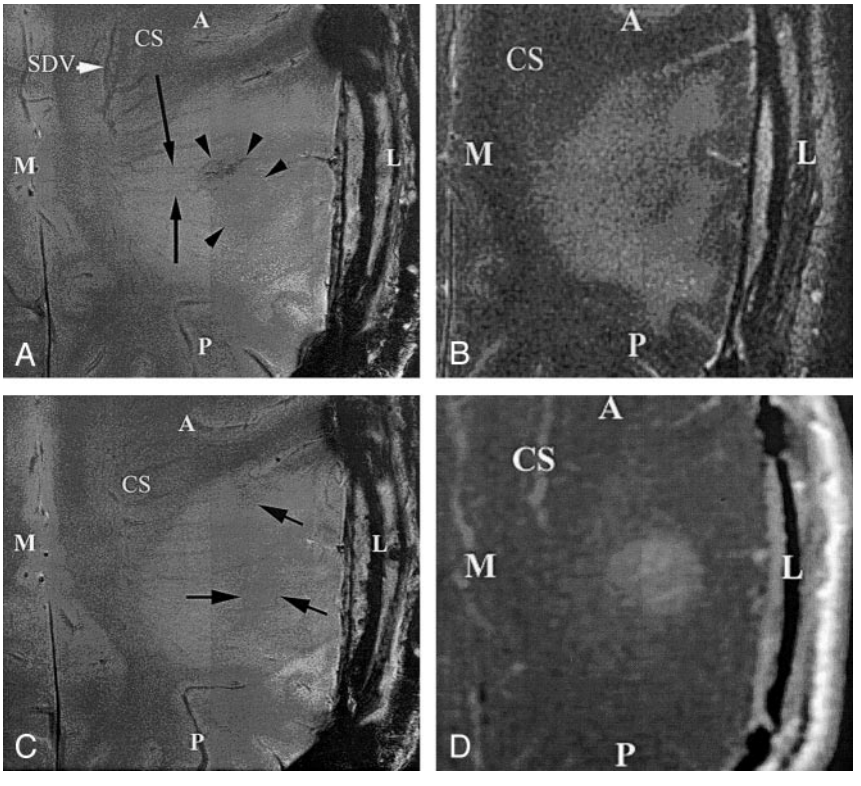

FIG 2. Axial images obtained through the superior aspect in patient with a glioblastoma multiforme demonstrate the ability to identify the fine angioarchitecture associated with the tumor at 8 T but not at 1.5 T. Note the enlargement and tortuosity of the transmedullary veins coursing over the tumor bed (*long arrows*), as compared with those in a healthy patient. The signal-intensity voids in the tumoral bed connect to the transmedullary veins (*short arrows*). Also note the area of overall decreased signal intensity that is associated with haphazardly arranged vessels, which are thought to represent neovascularity (*arrowheads*). *A* indicates anterior; *CS*, centrum semiovale; *L*, lateral; *M*, medial; *P*, posterior; *SDV*, subependymal draining vein.

A, Image obtained at 8 T (714/10, 23° flip angle, 900 × 900 matrix, 2-mm section thickness, 20-cm FOV).

B, FSE T2-weighted 1.5-T image (5650/104, 512 × 512 matrix, 3-mm section thickness, 20-cm FOV).

C, Image obtained at 8 T at one section superior to that in *B* (714/10, 23° flip angle, 900 × 900 matrix, 2-mm section thickness, 20-cm FOV).

D, Gadolinium-enhanced T1-weighted magnetization transfer images (616/20, 256 × 256 matrix, 5-mm section thickness).

findings on the 8-T images. Vessels identified with both techniques were also compared for the spatial resolution of vascularity.

A low signal-to-noise ratio was achieved at 1.5 T imaging by using a 2-mm section thickness, a 512 × 512-pixel matrix, and gradient-echo sequences similar to those used for 8-T imaging in this study. As a result, we could not reasonably compare the gradient-echo images obtained at 8 T with those acquired at 1.5 T (8). Therefore, 1.5-T FSE T2-weighted images were compared with 8-T gradient-echo 900 × 900 images.

Essentially all of the blood vessels were seen as hypointense regions without phase-encoded artifacts. Areas of disturbed vasculature in the tumoral bed were identified on 8-T MR images. These areas included enlargements of the adjacent transmedullary venous vasculature, irregularly shaped serpiginous signal-intensity voids in the tumoral bed, and foci of decreased signal intensity in the tumoral bed (Fig 2A). The irregularly shaped signal-intensity voids were connected to the transmedullary veins and were therefore believed to represent tumoral veins (Fig 2). When we compared the size of the tumoral vessels with that of the cortical penetrating veins in this patient, the tumoral vessels appeared larger and more tortuous (Fig 2). The ratio of the sums of the diameters of three transmedullary veins adjacent to the tumoral bed to three transmedullary veins away from the tumor bed was 1.8. This determination was not possible with the 1.5-T images; we could not identify the presence of irregular vessels in the tumoral bed on the 1.5-T images. Foci of decreased signal intensity were identified adjacent to the areas of increased vascularity on 8-T images (Fig 2A).

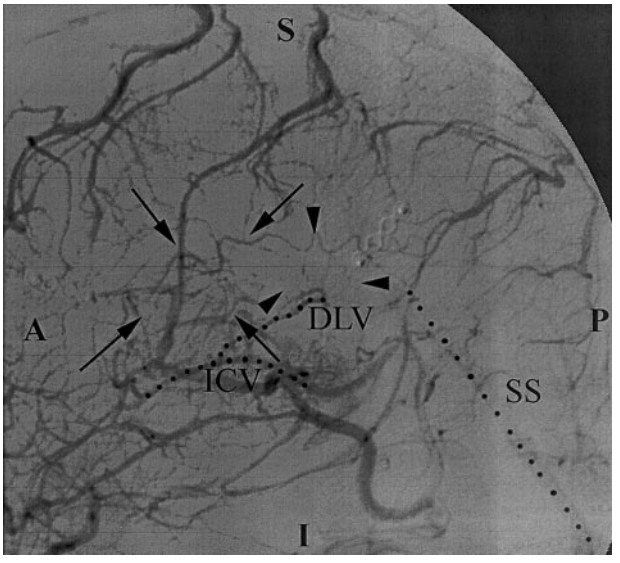

FIG 3. Lateral arteriogram obtained with a left carotid injection demonstrates tortuous vascularity (*arrows* and *arrowheads*) in the tumor bed within the glioblastoma multiforme. These findings were also identified on the 8-T images (Figs 1 and 2). However, the normal transmedullary veins and the smaller vessels are less conspicuous on DSA images than on 8-T images. *A* indicates anterior; *DLV*, direct lateral vein; *I*, inferior; *ICV*, internal cerebral vein; *P*, posterior; and *SS*, straight sinus.

The comparison of 8-T MR high-spatial-resolution images to DSA images revealed that both techniques were able to depict irregular vessels in the tumoral bed as well as enlarged transmedullary veins that drained the tumor. Regions of decreased signal intensity in the tumoral bed, which accompanied areas of increased vascularity at 8 T, corresponded to areas of vascular blush in the tumoral bed. Some of the larger transmedullary veins that drained the tumoral bed could be identified on conventional angiograms. However, the normal transmedullary veins identified on 8-T images were not visible on conventional angiograms. In addition, some of the smaller vascular structures in the tumoral bed that were depicted at 8 T were not identified on DSA images (Fig 3).

Discussion

Imaging with higher magnetic fields is associated with higher signal-to-noise ratios (9, 10). As such, high-quality imaging is possible with larger matrices, thinner sections, and faster acquisition times. Signal intensity can be lost with high field strengths because of increased magnetic susceptibility artifacts associated with the skull base, air spaces, and paramagnetic substances; longer T1 times; and shorter T2 and T2* times (9, 11). Unlike spin-echo imaging that suppresses local field inhomogeneities, the use of gradient recalled-echo imaging with a relatively long TE is sensitive to structures that containing notable concentrations of paramagnetic materials (9, 11, 12). These materials should include deoxyhemoglobin in venous blood and iron in deep gray matter nuclei. On the other hand, the magnetic susceptibility effects produced with gradient recalled-echo imaging become increasingly visible (lower signal intensity) as the TE increases. This effect leads to substantial geometric distortion of images acquired near the air spaces in the skull base (9, 11). In general, the images produced by using the parameters in this study showed little distortion with the exception of structures adjacent to the skull base. Because intracranial arterial and venous vasculature can appear as flow voids on 8-T MR images obtained with intermediate TEs (8–20 m), we were not able to discriminate between these two types of vessels with means other than anatomic location (12). The higher deoxyhemoglobin content of the venous structures is believed to account for the visibility of the smaller venous structures (12).

The angioarchitecture and perfusion of a tumor is known to differ from those of normal brain. Vessels in the tumoral bed are more tortuous, larger, and more disorganized (13). The microvasculature in rat gliomas are 2–3 times as large as those in normal cortex, and the vessel diameters may be as large as 250 μm (13). These dimensions are well within the range of the resolution at 8-T imaging.

High-field-strength MR imaging at 8 T with a large matrix enables visualization of the vasculature to approximately 100 μm (12). This type of high-resolution imaging enabled us to directly identify vascular features in the tumoral bed in this case. The 8-T MR imaging findings in the tumor related to vascular distortion included enlargement and tortuosity of transmedullary veins adjacent to the tumor and foci of increased vascular density in the tumoral bed. Results of previous studies have demonstrated that apparent vascular density in a nude-mouse glioma model, as identified on 4.7-T gradient-echo MR images, is significantly correlated with the histopathologically identified density of blood-containing vessels (6). High-resolution MR imaging of apparent vascular density has been successfully used as an assay for angiogenesis in this same animal model (6, 7). Therefore, the identification of the neovascularity in brain tumors should be possible with 8-T MR imaging. In these studies, vascular density was quantified from the signal intensity loss in susceptibility-weighted images due to the paramagnetic property of deoxyhemoglobin (5–7). This vascular density determination may help to supplement the direct visualization of tumoral microvasculature by representing vascular structures with sizes beyond the resolution of 8-T imaging. However, this possibility remains to be studied in humans.

The angiographic appearance and vascular pattern of glioblastoma have previously been described as varying widely and not consistently present (14, 15). Typically, glioblastoma neovascularity is characterized by a pattern of increased vascularity in which the vessels are irregularly arranged with alternating foci of dilatation and constriction. The draining veins are dilated, they often appear on arterial-phase angiograms, and they are indications for shunt surgery (14, 15). These angiographic features of neovascularity are reminiscent of the microvascular features identified at 8 T in this case in this report. Preliminary evidence thus

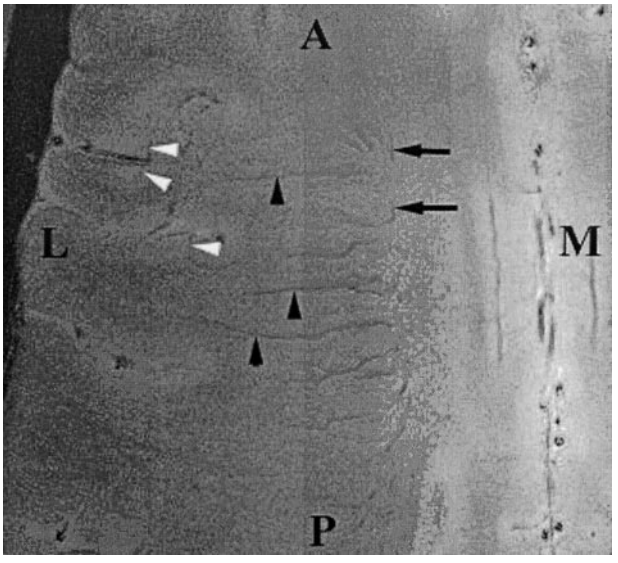

FIG 4. Axial gradient-echo 8-T MR images (600/12, 23° flip angle, 2-mm section thickness, 1024 × 1024 matrix, 20-cm FOV) display the medullary veins in the head of a healthy volunteer. The image is centered at the centrum semiovale and shows many transmedullary veins (*black arrowheads*) that drain into the subependymal veins (*arrows*), which are depicted as linear signal intensity voids converging on the surface of the lateral ventricles. Also note the cortical penetrating veins (*white arrowheads*). *A* indicates anterior; *L*, lateral; *M*, medial; and *P*, posterior.

far indicates that the resolution of venous vasculature may be higher with imaging at 8 T or the same as that of other techniques. In our experience, the transmedullary veins were consistently identified on 8-T gradient-echo 1024 × 1024 images (Fig 4) (12) but not on conventional angiograms (14, 15). In addition, several small branches of the transmedullary veins that were identified with 8-T imaging were not clearly identified with DSA (Fig 2).

The current study provides preliminary evidence that direct visualization of microvascularity within a glioblastoma multiforme may be possible at 8 T. This possibility supports endeavors to further examine whether this tumoral microvascularity may indeed represent neovascularity. The consistency of these findings should be confirmed in a larger population of patients.

Acknowledgment

We wish to acknowledge Dr Pierre-Marie Robitaille, whose persevering efforts allowed for the development and function of 8-T MR imaging

References

1. Kleihues P, Burger PC, Plate KH, Ohgaki H, Cavanee WK. **Glioblastoma.** In: Kleihues P, Cavenee WK, eds. *Pathology and genetics of Tumours of the Nervous System.* Lyon: International Agency for Research on Cancer; 1997:22
2. Brem S, Cotran R, Folkman J **Tumor angiogenesis: a quantitative method for histologic grading.** *J Natl Cancer Inst* 1972;48: 347–356
3. Weidner N. **Tumoral vascularity as a prognostic factor in cancer patients: the evidence continues to grow.** *J Pathol* 1998;184:119–122
4. Eberhard A, Kahlert S, Goede V, Hemmerlein B, Plate KH, Augustin HG. **Heterogeneity of angiogenesis and blood vessel maturation in human tumors: implications for antiangiogenic tumor therapies.** *Cancer Res* 2000;60:1388–1393
5. Abramovich R, Marikovsky M, Meir G, Neeman M. **Stimulation of tumour angiogenesis by proximal wound: spatial and temporal analysis by MRI.** *Br J Cancer* 1998;77:440–447
6. Abramovich R, Meir G, Neeman M. **Neovascularization induced growth of implanted C6 glioma multicellular spheroids: magnetic resonance microimaging.** *Cancer Res* 1995;55:1956–1962
7. Neeman M. **Preclinical MRI experience in imaging angiogenesis.** *Cancer Met Rev* 2000;19:39–43
8. Burgess RE, Yu Y, Christoforidis GA. **Human Leptomeningeal and cortical vascular anatomy of the cerebral cortex at 8 Tesla.** *J Comp Assist Tomogr* 1999;23:850–856
9. Abduljalil AM, Kangarlu A, Yu Y, Robitaille PML. **Macroscopic susceptibility in ultra high field MRI, II: acquisition of spin echo images from the human head,** *J Comput Assist Tomogr* 1999;23: 842–844
10. Vaughan JT, Garwood M, Collins CM, et al. **7T vs. 4T: RF power, homogeneity, and signal-to-noise comparison in head images.** *Magn Reson Med* 2001 Jul;46(1):24–30
11. Abduljalil AM, Robitaille PML. **Macroscopic susceptibility In ultra high field MRI.** *J Comput Assist Tomogr* 1999;23:832–841
12. Christoforidis GA, Bourekas EC, Baujan M, et al. **High resolution MRI of the deep brain vascular anatomy at 8 tesla: susceptibility-based enhancement of the venous structures.** *J Comput Assist Tomogr* 1999;23:857–866
13. Zama A, Tamura M, Inoue H. **Three-dimensional observations on microvascular growth in rat glioma using a vascular casting method.** *J Cancer Res Clin Oncol* 1991;117:396–402
14. Huang YP, Wolf BS. **Veins of the white matter of the cerebral hemispheres (the medullary veins): Diagnostic importance in carotid angiography.** *Am J Roentgenol Radium Ther Nucl Med* 1964; 92:739–755
15. Wickborn, I. **Tumor circulation.** In: Newton TH, Potts GD, eds. *Radiology of the Skull and Brain: Angiography—Specific Disease Processes.* St Louis: Mosby; 1974:2257–2285